Bankline Shifting and Sand Bar Dynamics of the Teesta River Using Multi-Temporal Satellite Images

Md. Sazedur Rahman[1], S M Ahsan Habib[2*], Md. Jahidul Ashik[2], Muhammad Sharif[2] and M Nur Hossain Sharifee[2]

[1]Department of Water Resources Engineering, Bangladesh University of Engineering and Technology (BUET), Dhaka 1000, Bangladesh
[2]Bangladesh Space Research and Remote Sensing Organization (SPARRSO), Dhaka 1207, Bangladesh

Manuscript received: 20 April 2025; accepted for publication: 14 October 2025

ABSTRACT: The Teesta River, a major transboundary watercourse in northern Bangladesh, has undergone pronounced geomorphological transformations under the influence of both natural hydrological variability and human interventions. This research explores the spatial and temporal evolution of bankline migration and sandbar formation between 1996 and 2023 using multi-temporal Landsat MSS, TM, and OLI imagery integrated with an area-based Geographic Information System (GIS) framework. The approach, which quantifies total areal changes in erosion and deposition rather than linear displacement, provides a more comprehensive representation of morphodynamic adjustments within a braided river environment. Eight cloud-free satellite epochs were analyzed across a 112 km reach between Khoga Khoribari and Haripur Ghat, complemented by discharge and water-level data from the Dalia and Kaunia stations of the Bangladesh Water Development Board. The findings indicate significant channel widening, with mean left-bank erosion of -2.60 km² per year and right-bank deposition of 1.02 km² per year, resulting in an overall widening rate of 1.58 km² annually. Total sandbar area showed a net accretion of 3.17 km² per year, mainly from temporary bars (3.64 km² per year), while permanent bars experienced a slight loss (−0.47 km² per year), signifying a shift toward a more braided and unstable channel form. The downstream section (Section 4) emerged as the most active reach, exhibiting the highest erosion and deposition magnitudes (-16.4 and 8.98 km² per year, respectively). Correlation analysis revealed strong coupling between discharge and river area (r = 0.52) and between river area and sandbar area (r = 0.88), underscoring the dominance of hydrological forcing in shaping morphological responses. Overall, the study highlights the increasing morphological instability of the Teesta River and its implications for floodplain livelihoods and infrastructure planning. The area-based GIS technique demonstrates superior capacity to capture the volumetric complexity of erosion deposition processes, offering valuable insights for sustainable river management, sediment control, and adaptive basin planning across monsoon-driven deltaic systems.

Keywords: Teesta River; Deposition; Erosion; Sandbars; Bank Line Shifting; Landsat; GIS

INTRODUCTION

Rivers in monsoon-dominated deltaic environments exhibit exceptional morphological dynamism, governed by the interactions between hydrological variability, sediment flux, and anthropogenic modifications. Within the Ganges-Brahmaputra-Meghna (GBM) basin, one of the world's largest and most sediment-laden river systems, the continuous interplay of erosion, accretion, and channel migration shapes the landscape of Bangladesh. The country's extensive floodplain network, encompassing over 900 rivers (57 of which are transboundary), underpins its agricultural productivity, fisheries, and navigation systems, while also sustaining millions of livelihoods (Pandit et al., 2024; Lee-Ammons & Riosmena, 2019). Yet, these same dynamic fluvial processes also pose persistent challenges, including riverbank erosion, floodplain instability, and sandbar (char) dynamics, which lead to significant land loss, displacement, and socio-economic vulnerability (Darby et al., 2010; Islam et al., 2020).

Among the major GBM tributaries, the Teesta River plays a pivotal role in the hydrology and economy of northern Bangladesh. Originating from the Pauhunri Glacier in the eastern Himalayas, the Teesta traverses India's Sikkim and West Bengal states before entering Bangladesh, where it supports irrigation, agriculture, and domestic water supply across Rangpur,

Corresponding author: S M Ahsan Habib
E-mail: ahsn_env@yahoo.com

DOI: https://doi.org/10.3329/dujees.v14i2.87591

Lalmonirhat, Nilphamari, Kurigram, and Gaibandha districts (Mandal & Chakrabarty, 2016). However, the river's natural hydrological regime has been significantly altered by hydraulic infrastructures, notably the Gajoldoba Barrage in India and the Teesta Barrage Project (TBP) in Bangladesh. These structures have disrupted downstream flow patterns, reducing dry-season discharge by up to 60% and amplifying wet-season floods exceeding 3,500 m^3/s (Das et al., 2022). Such alterations have intensified bank line migration, sediment aggradation, and morphological instability, leading to severe erosion, flood hazards, and livelihood insecurity in the floodplain (Tarannum et al., 2018; Sultana, 2022).

The morphodynamics of the Teesta, like other Himalayan-fed rivers, are characterized by alternating phases of erosion and deposition controlled by monsoonal hydrology and sediment transport (Lawler et al., 1997; Archana et al., 2012; Azuma et al., 2007). Studies on the Brahmaputra, Jamuna, and Ganges rivers have revealed bank retreat rates exceeding 100 m/yr in braided reaches, often linked to peak monsoonal flows and reduced sediment cohesion (Baki & Gan, 2012; Gao et al., 2021). Anthropogenic interventions such as flow regulation, embankment construction, and sediment trapping further modify discharge regimes and sediment delivery, driving downstream instability (Hackney et al., 2017). In the Teesta basin, these processes manifest as frequent channel migration, asymmetric bank line behavior, and recurrent sandbar reformation that collectively reshape the floodplain landscape (Baki et al., 2022; Islam et al., 2020). Persistent erosion erodes fertile land and displaces communities, while newly accreted chars are often unstable and unsuitable for long-term settlement, amplifying socio-economic inequality across riparian populations (Lee-Ammons & Riosmena, 2019).

Over the past three decades, remote sensing (RS) and geographic information systems (GIS) have emerged as powerful tools for quantifying river morphodynamics. Multi-temporal satellite datasets, particularly from the Landsat series, allow consistent, objective, and cost-effective monitoring of bank line shifts, channel width variations, and sandbar evolution at regional scales (Baki & Gan, 2012; Takagi et al., 2007; Bhakal et al., 2005). For the Teesta River, several studies have employed RS–GIS methods to characterize planform change and predict migration trends (Akhter et al., 2019; Parvej et al., 2024; Islam & Guchhait, 2024). However, many of these efforts rely on transect-based linear approaches, such as the Digital Shoreline Analysis System (DSAS), which measures bank displacement along fixed cross-sections. While suitable for single-thread channels, these models can underrepresent true change in braided rivers like the Teesta, where channels continuously bifurcate and remerge (Parsons et al., 2022; Dutta et al., 2018). Other works have incorporated autoregressive or ARIMA modeling (Akhter et al., 2019) and structural impact assessments (Uddin et al., 2024), but often neglect to calculate area-based channel and sand bar migration with explicit integration of hydrological parameters such as discharge and stage variability, key drivers of short-term morphological response.

To address these limitations, area-based GIS analysis provides a more holistic alternative. Rather than measuring displacement along predefined transects, it calculates total areal changes in erosion and accretion between consecutive time intervals, effectively capturing both lateral and vertical adjustments (Baki & Gan, 2012; Yang et al., 2021). This method is particularly advantageous in braided systems, where planform variability and bar mobility dominate (Dutta et al., 2018). When combined with hydrological datasets, such as discharge and water-level records, area-based approaches enable the assessment of the coupling between hydrological forcing and geomorphic adjustment, thereby improving the predictive understanding of sediment redistribution and channel behavior (Moody, 2022; Malcolm et al., 2012).

The Teesta River provides a compelling case study for such integrated analysis. Its highly dynamic braided morphology, strong monsoonal influence, and history of flow regulation make it a critical system for assessing interactions between natural and anthropogenic controls on river evolution. Moreover, its socio-economic significance magnifies the urgency for data-driven, spatially explicit morphodynamic assessment. Recurrent left-bank erosion, estimated at several square kilometers per year, causes extensive loss of agricultural land and infrastructure, while unstable depositional bars continue to reshape settlement patterns (Islam et al., 2020; Baki et al., 2022).

This study, therefore, aims to quantify the spatiotemporal evolution of bank line shifting and sandbar dynamics of the Teesta River between 1996 and 2023 using

multi-temporal Landsat imagery integrated within an area-based GIS framework. The specific objectives are to: (i) measure erosion and accretion rates along the riverbanks; (ii) examine temporal variations in temporary and permanent sandbars; (iii) identify reach-specific morphodynamic activity; and (iv) explore the correlation between discharge fluctuations, water level, and channel behavior. By emphasizing areal change over linear displacement, this work offers a comprehensive depiction of morphodynamic evolution in a braided, monsoon-driven river system.

Beyond its scientific contribution, this research provides actionable insights for sustainable floodplain management, sediment budgeting, and transboundary river governance. The methodological framework demonstrated here, which integrates remote sensing, GIS, and hydrological correlation, offers a transferable model for other large alluvial rivers in South Asia, where climatic extremes and infrastructure development are increasingly reshaping fluvial landscapes.

DATA AND METHODS

Study Area and Data Collection

The Teesta River, located in the northern region of Bangladesh, is the fourth largest river system in the country and is known for its vigor, often referred to as the lifeblood of Bangladesh's north (Fig. 1). The river spans 129 km within Bangladesh, with a channel width ranging from 0.7 km to 5.5 km and an average width of 3 km. Its left bank elevation decreases from 57.10 m upstream to 18.37 m downstream, while the right bank ranges from 56.18 m to 19.00 m, and the riverbed slopes from 54.00 m to 16.74 m, reflecting significant potential for sediment transport and morphological changes (BWDB, 2011). Approximately 14% of Bangladesh's agricultural land is situated along rivers, supporting the livelihoods of over 21 million people, or 7.3% of the nation's population, who are directly or indirectly reliant on these waterways (Lee-Ammons & Riosmena, 2019).

It passes through the five districts that make up the Rangpur Division in Bangladesh: Gaibandha, Kurigram, Lalmonirhat, Nilphamari, and Rangpur districts (Lee-Ammons and Riosmena, 2019). The region's floodplain comprises the Teesta and several other small and medium-sized rivers. Every year during the flood season, this river dumps sediments that make the plain fertile and are conducive to cultivation (Mandal and Chakrabarty, 2016). The total Teesta River is about 414 km and originates in the Pauhunri Mountain in the eastern Himalayas, till it meets the Brahmaputra River in Bangladesh and flows through. For our study purpose with the social, economic, scientific, and cultural interest of Bangladesh, the selected reach is about 112 km long only in Bangladesh that starts from Khoga Khoribari, Dimla Upazila, Nilphamari District, and ends at Haripur Ghat, Sundarganj Upazila, Gaibandha District. The total area is divided into 4 sections from upstream to downstream (Fig. 1) according to the bend for precise analysis and understanding of the spatial morphodynamics

In this study, freely available satellite images were obtained from the United States Geological Survey (USGS) database https://earthexplorer.usgs.gov at a spatial resolution of 30 meters. Eight Landsat image sets from 1996, 1999, 2003, 2006, 2011, 2015, 2019, and 2023 were selected to examine post-1995 flood-induced morphological adjustments and the subsequent changes after the Teesta barrage construction up to the most recent Landsat 8 observations. All images, having the same path and row, were downloaded in GeoTIFF format, requiring four tiles to cover the entire study area. The images were projected to the Universal Transverse Mercator (UTM) Zone 46N coordinate system based on the World Geodetic System (WGS) 1984. To ensure temporal consistency and minimal atmospheric interference, only daytime images with less than 14% cloud cover were selected, primarily from late November to early December (Table 1), coinciding with the dry season when hydrological conditions are relatively stable, comprehensive image pre-processing steps, such as radiometric calibration, atmospheric correction, and mosaicking were performed to ensure data uniformity and accuracy.

Hydrological data for monthly maximum and minimum discharge and water level records were collected from the Bangladesh Water Development Board (BWDB) at Dalia and Kaunia stations (Fig. 1) of the study period from 1996 to 2023 to make a correlation with the morphological study.

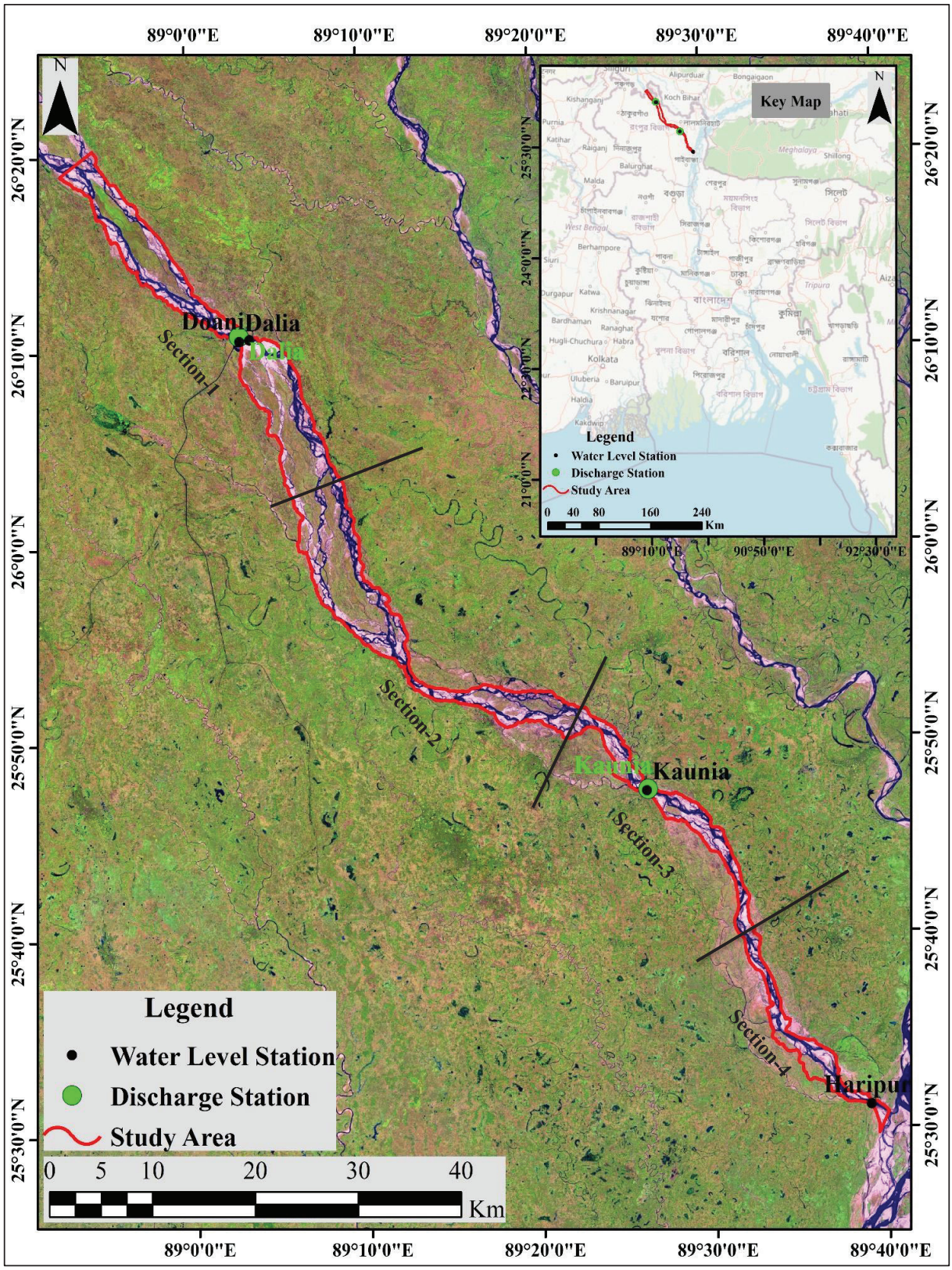

Figure 1: Map of the Study Area

Table 1: Landsat Satellite Images Used in the Present Study

Year	Version	Bands	Acquired Date
1996	Landsat-5		11/30/1996
1999	Landsat-5		12/25/1999
2003	Landsat-5	Band 1-Blue, Band 2-Green, Band 3- Red and Band 4-Near-Infrared	11/18/2003
2006	Landsat-7		12/05/2006
2011	Landsat-5		12/08/2011
2015	Landsat-8		11/19/2015
2019	Landsat-8	Band 2 – Blue, Band 3 – Green, Band 4 - Red, Band 5- Near-Infrared	11/14/2019
2023	Landsat-8		12/09/2023

Methodology

Image Pre-Processing and Extraction of Riverbanks and Sandbar Features

Landsat satellite images from 1996 to 2023 were processed in ArcGIS (version 10.8.2) following a structured workflow to analyze riverbank shifting and sandbar dynamics along the Teesta River. Raster datasets were first imported using the Add Data function, and multiple image tiles were merged into seamless spatial coverage using the Mosaic tool (Nie et al., 2023).

After mosaicking, image correction procedures were applied to enhance spectral accuracy and ensure consistency among multi-temporal datasets. Radiometric calibration converted raw digital numbers to surface reflectance values, eliminating sensor-related biases, while atmospheric correction reduced haze and scattering effects caused by atmospheric particles. These steps standardized the brightness and contrast of all images, allowing direct temporal comparison and improving the reliability of classification outputs.

Subsequently, non-referenced or partially referenced images were rectified using the Georeferencing toolbar by assigning accurately distributed Ground Control Points (GCPs) from stable landscape features visible on topographic maps and high-resolution Google Earth imagery. The affine transformation method was employed to refine spatial alignment, and the Root Mean Square Error (RMSE) was minimized to maintain positional accuracy across all image sets (Angel et al., 2020).

After correction and rectification, true-color composites were generated using the Composite Bands tool for initial visualization. The Clip tool was used to extract spatial subsets confined to the 112 km reach of the Teesta River within Bangladesh. Band stacking was performed to integrate multiple spectral layers into a single multiband raster, which facilitated land-cover classification and feature extraction (Ahmad et al., 2024; Bui et al., 2022).

Unsupervised image classification was then applied to differentiate surface features within the river corridor. This method was selected over spectral indices such as NDWI and NDVI because it better distinguishes mixed surfaces, shallow water, moist sand, and sparse vegetation, which are common in braided channels, where spectral overlap limits the performance of these indices. The classified outputs were subsequently reclassified into three geomorphic categories: (i) Water, representing the active channel; (ii) Sand/Bare land, representing temporary sandbars; and (iii) Cultivated/ Vegetated land, representing permanent sandbars. Similar approaches have been effectively used in large alluvial systems such as the Jamuna and Teesta Rivers (Baki & Gan, 2012; Akhter et al., 2019).

The reclassified rasters were converted to vector format using the Raster to Polygon tool, and the Feature to Polygon function was used to delineate continuous riverbank and sandbar polygons. Manual editing and topological checks ensured the removal of misclassified patches and the correction of mixed-pixel boundaries. Each extracted layer was verified against Google Earth imagery and field observations through a week's field visit covering the whole study area in both dry and monsoon seasons to confirm spatial and thematic accuracy.

All processing steps from mosaicking, correction, and georeferencing to classification and vector conversion were applied consistently across the eight temporal datasets (1996, 1999, 2003, 2006, 2011, 2015, 2019, and 2023) to ensure temporal uniformity and analytical comparability. The complete workflow is illustrated in Figure 2, summarizing the sequential operations from raw image preparation to final feature extraction. For clarity, only the exported bank lines of the selected downstream reach (Section 4) are displayed in Figure 3, as this reach exhibited the highest morphological activity. Although sandbar shapefiles were not displayed due to their geometric complexity, the process was the same for them; they were fully utilized in quantifying erosion, deposition, and sandbar evolution across the entire study period.

Erosional and Depositional Data Extraction and Analysis

Erosion and deposition dynamics were quantified in ArcGIS by superimposing two sets of polygons representing bank lines or sandbars for both sets from consecutive years, such as 1996 and 1999, or 1999 and 2003. The Union tool was applied to overlay the polygons, enabling the detection of eroded and accreted zones through spatial change detection. Polygonal areas corresponding to erosion, deposition, and common areas were then calculated using the Calculate Geometry function in the attribute table. Final outputs were visualized through map creation to illustrate spatial patterns of erosion, deposition, common areas, and channel dynamics over the study period, as shown in Figure 4.

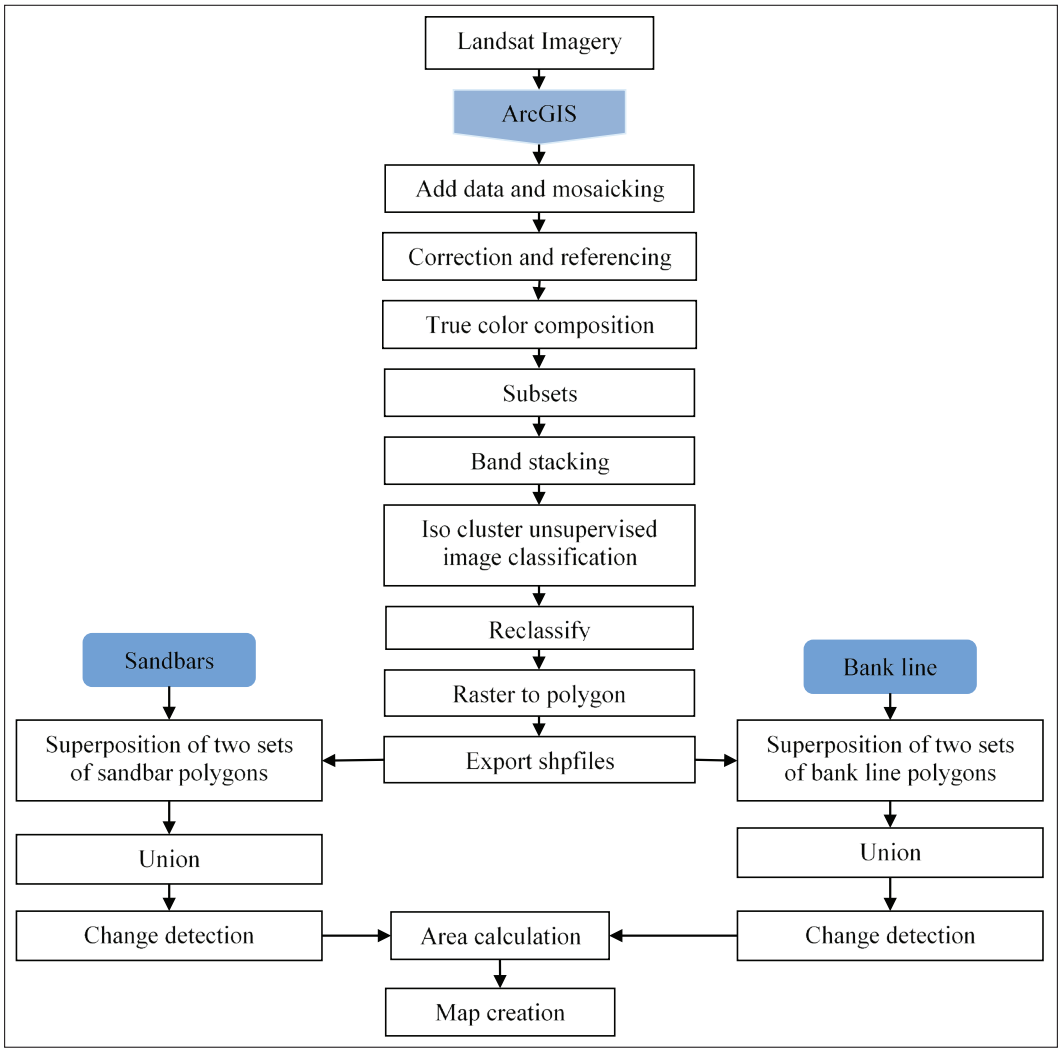

Figure 2: Workflow of Research Methodology

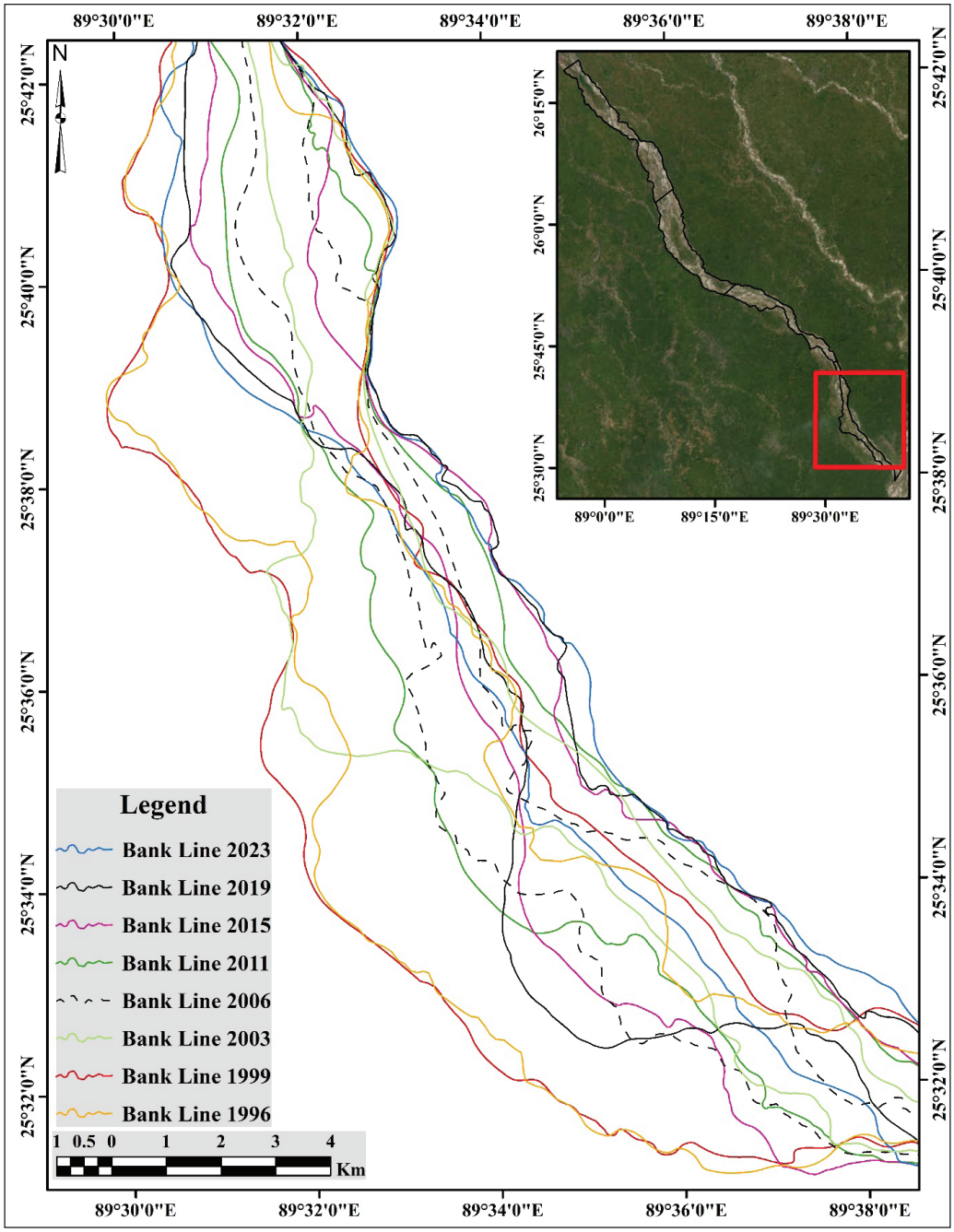

Figure 3: The Exported Bank Lines of the Teesta River from 1996 to 2023

Only a small part of Section 4 was shown in this figure for one interval, 2003-2006, of bank lines, as bank lines are more explicit to understand and visualize, rather than sand bars, but a similar procedure was applied for sandbar area calculations and presentation.

Based on these output areas, the shifting rates of bank lines and sandbars were estimated using Eq. (1) from the Microsoft Excel application

$$R = \frac{A_1 - A_2}{Y} \quad \ldots\ldots\ldots\ldots\ldots (1)$$

where R (km²/year) denotes the erosional or depositional shifting rate, A_1 (km²) represents deposition, and A_2 (km²) represents erosion, and Y (years) denotes the time interval between two adjacent datasets. Accordingly, positive values of $A_1 - A_2$ indicated net deposition, while negative values indicated net erosion.

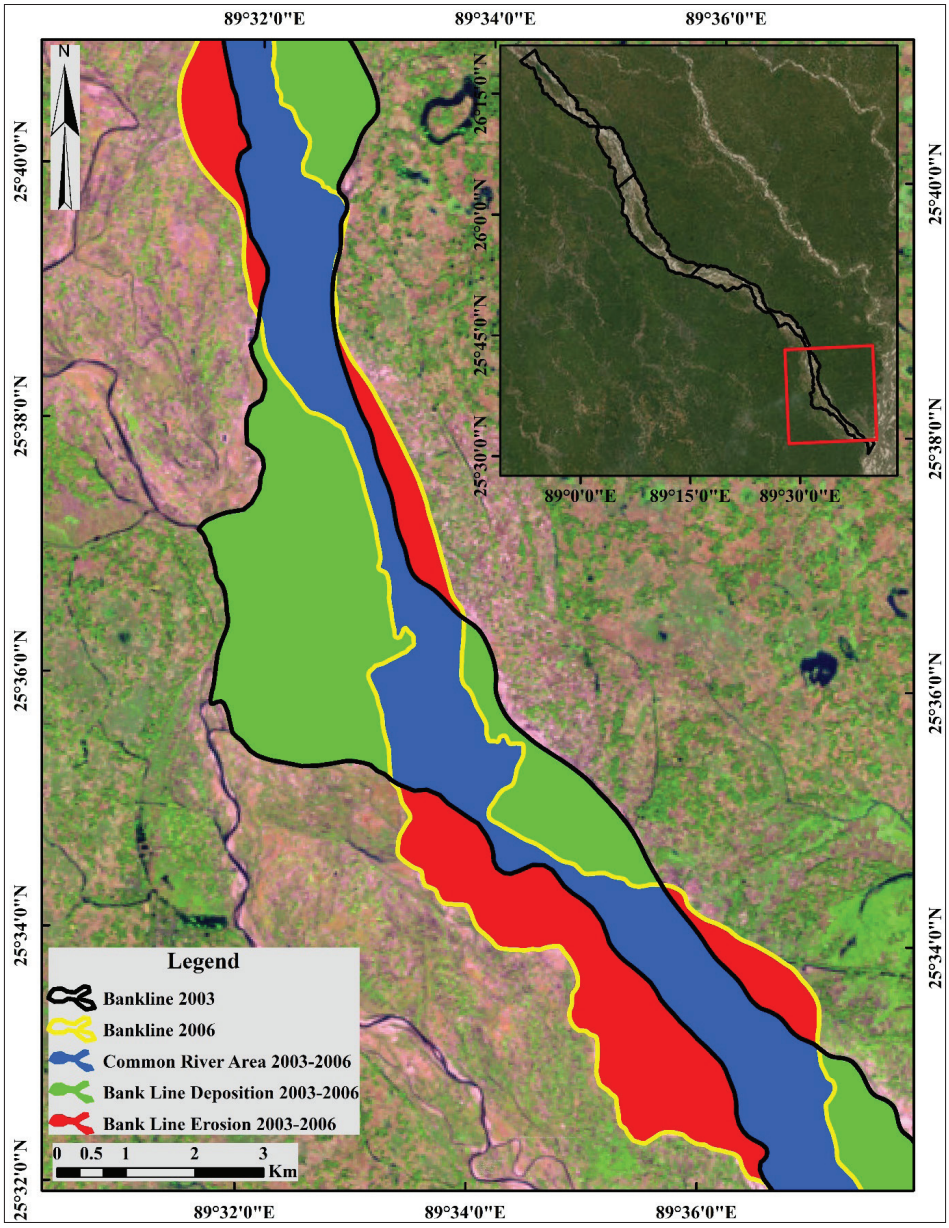

Figure 4: The Teesta River's Bank Line Erosion and Deposition from 2003 to 2006

Relation Between Extracted Hydraulic and Hydrologic Data

To explore the interaction between river morphology and hydrological drivers, a correlation analysis was conducted between the extracted hydraulic variables (River area, Permanent Sandbars area, total sandbars area, and temporary sandbars area) and the observed hydrological parameters (water level and discharge at Dalia and Kaunia gauging stations, as shown in Fig. 1). This analysis was intended to quantify the dependency of morphological adjustments on flow dynamics and to evaluate their implications for water resource management.

The statistical relationship was measured using the Pearson correlation coefficient (Mahmud et al., 2021), expressed in Eq. (2), with the help of a scatter plot in the Microsoft Excel application

$$r = Correl(X,Y) = \frac{\sum(x-\bar{x})(y-\bar{y})}{\sqrt{\sum(x-\bar{x})^2 \sum(y-\bar{y})^2}} \ldots\ldots\ldots(2)$$

Where r was the correlation value, x was the hydraulic data (River area, Permanent Sandbars area, total sandbars area, and temporary sandbars area) for different analyses and $\bar{x}$ was the average of x. Here, y was the hydrologic data (water level and discharge of Dalia and Kaunia points) for different analyses, and $\bar{y}$ was the average of y.

Hydrologic parameters such as discharge and water level acted as governing forces for hydraulic processes, as they regulated sediment entrainment, transport, and subsequent deposition. Variations in discharge, particularly during peak flow events, increased shear stress along the riverbanks, enhancing erosion potential, while lower flows facilitated sediment deposition and bar formation (Gao, Li, & Yang, 2021; Moody, 2022). Establishing a statistical correlation between hydrologic and hydraulic datasets ensured a better understanding of river dynamics and provided critical inputs to hydraulic understanding. These insights were vital for predicting channel behavior and dynamic alluvial systems (Malcolm et al., 2012).

RESULTS

Temporal Variations of River and Sandbar Area (1996–2023)

The analysis of the Teesta River's area and sandbar dynamics from 1996 to 2023 revealed considerable spatial and temporal variability, as shown in Figure 5. The river area fluctuated between 322.77 km² (1996) and 389.10 km² (1999), with an overall average of 354.98 km², reflecting a gradual widening of the channel. The total sandbar area (Permanent and temporary) exhibited a similar dynamic, with values ranging from 256.56 km² to 344.97 km² and an average of 289.34 km², peaking in 1999 when both river area and sandbar extent reached their maxima. Permanent sandbars remained relatively stable throughout the study period (average 122.30 km²), though their long-term trend indicates localized erosion and a gradual reduction in areal coverage. In contrast, temporary sandbars displayed strong interannual variability, ranging from 128.84 km² to 223.97 km² with an average of 168.05 km², highlighting their high sensitivity to seasonal hydrologic fluctuations and flood-induced sediment redistribution.

The year 1999 stood out as a critical phase, marked by the largest extent of both river area and sandbar coverage, particularly temporary sandbars, which were likely linked to elevated monsoonal discharge and morphological adjustments following the post-operation of the Teesta Barrage. Subsequent years (2011 and 2019) also recorded notable expansions in temporary sandbars, underscoring their role as the principal driver of total sandbar variability. Overall, the findings indicated that while the Teesta River has progressively widened, its bar morphology remains highly dynamic, dominated by temporary sandbars that modulate the geomorphic response to hydrological variability and discharge extremes.

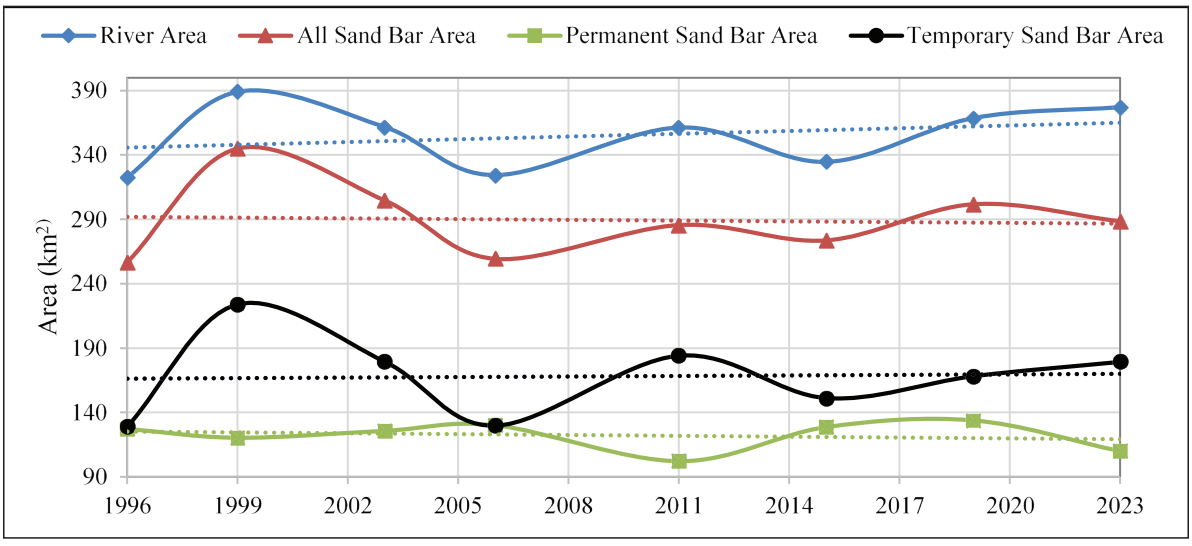

Figure 5: Variation of River and Sand Bars Area during the Study Period

Sandbar Dynamics and Morphological Transition of the Teesta River

The sandbar analysis revealed a pronounced transformation in the Teesta River's bar morphology, as illustrated in Figure 6. Over the study period, the total sandbar area exhibited a net accretion rate of 3.17 km²/year, largely driven by the expansion of temporary sandbars (+3.64 km²/year). In contrast, permanent sandbars displayed a modest net decline (−0.47 km²/year), suggesting a transition toward a system increasingly dominated by unstable, short-lived depositional features.

This evolving pattern can be attributed to two contrasting yet interrelated processes. First, large depositional pulses such as the significant gross deposition of 31.7 km²/year during 1996–1999 triggered rapid sandbar growth and the proliferation of temporary bars, thereby inflating the total sandbar area. Second, intense erosional episodes, notably the −16.53 km²/year loss during 2003–2006, revealed how these newly formed bars were later dismantled or reworked by high-energy flood events. These alternating depositional and erosional cycles, particularly evident in the late 1990s (coinciding with barrage construction and operational adjustments) and recurring peaks in 2011 and 2019, underscore that the Teesta's bar dynamics are primarily governed by episodic hydrological forcing rather than gradual, long-term accretionary processes.

From a geomorphological perspective, the contrasting trends between temporary and permanent sandbars indicate a major morphological transition in the Teesta River. The decline of permanent bars has reduced long-term channel stability, while the rise of temporary bars has increased braid-channel complexity and short-term variability. As a result, sediment routing is now dominated by transient storage, making the system highly responsive to flood events and prone to rapid channel reorganization. This dynamic behavior not only complicates river management and flood control but also reduces the economic utility of sandbars and contributes to greater erosion risk along the riverbanks.

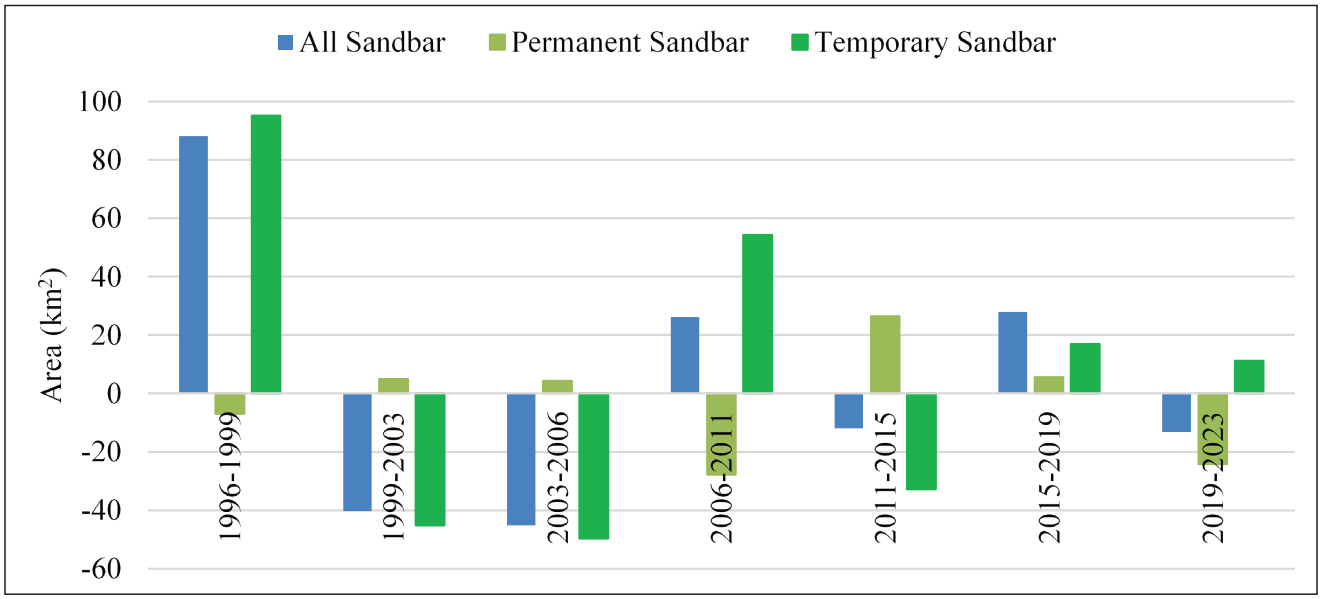

Figure 6: Changes in Sandbar Areas

Section-wise Dynamic Behavior of Riverbank and Sandbars during the Study Period

For better understanding, the total study area was divided into four sections, as stated before, and is shown in Figure 1. Sectional analysis identified that Section 4 (downstream reach) was the most dynamic, followed by Section 2; Section 3 was the most stable of the four reaches. Section-scale extremes, including maximum net deposition of 8.98 km²/yr in Section 2 (1999–2003) and severe erosion concentrated in Section 4 (e.g., −16.4 km²/yr for all sandbars (1999–2003) as shown in Figure 7.

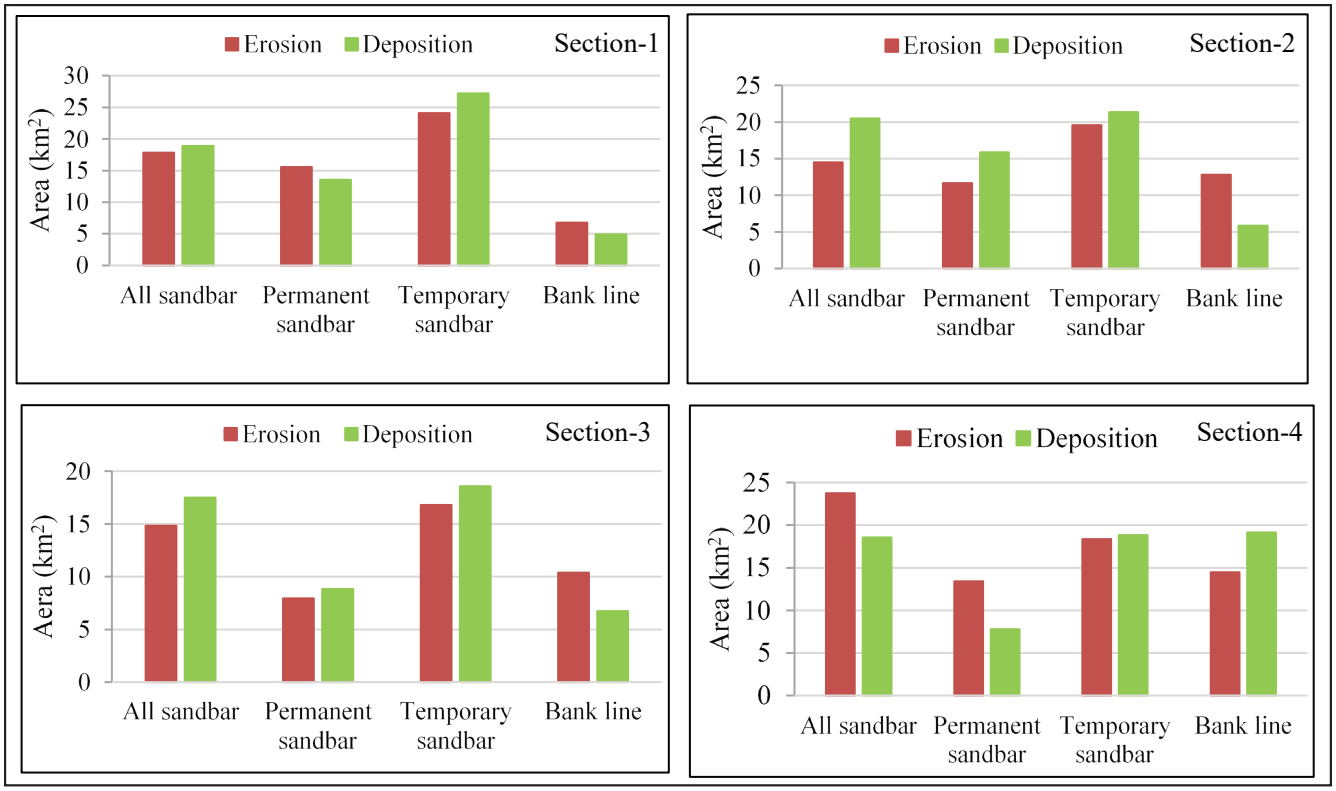

Figure 7: Deposition and Erosion Statistics of Four Sections for the whole Study Period

This spatial hierarchy of dynamism reflects interacting controls: downstream reaches (Section 4) concentrated flow energy and incoming sediment flux, so they experienced larger magnitudes of both erosion and deposition; mid-reach bends (Section 2) appeared sensitive to alternating cut-and-fill cycles, producing large standard deviations in bar and bank change. Conversely, the low variability in Section 3 suggests local factors (lower slope, cohesive banks, vegetation, or anthropogenic protections) that dampened bar migration and bank retreat.

From an analytical perspective, it was shown that the Teesta was not uniformly active; therefore, management must be spatially targeted. High variability in Sections 4 and 2 implies prioritized monitoring and adaptive bank protection where rapid lateral change threatens infrastructure and farmland. Consideration of how interventions (e.g., local dykes, dredging) in one section can redistribute energy and sediment to downstream reaches, potentially amplifying instability there.

Asymmetric Bankline Migration and Channel Widening Trends

Bank-line migration was strongly asymmetric: the left bank showed net erosion of −2.60 km²/yr while the right bank recorded net deposition of +1.02 km²/yr, yielding an overall river widening of 1.58 km²/yr. Peak short-term rates were extreme left-bank values, including accretion of +10.49 km²/yr (2003–2006) and erosion of −11.25 km²/yr (1996–1999); the right bank saw accretion of up to +17.39 km²/yr (1999–2003), as shown in Figure 8.

These asymmetric patterns pointed to two interacting drivers. First, hydraulic forcing and channel curvature concentrated shear stress on the left bank (hence persistent net erosion), while morphological controls and localized protections on the right bank favored net deposition. Second, episodic hydrologic events (monsoonal discharge peaks and post-barrage adjustments) generate brief intervals of very high bank mobility that dominate long-term area-based migration metrics. Sectional extremes (e.g., left-bank maximum erosion −10.35 km²/yr in Section 2; right-bank peak

deposition +15.88 km²/yr in Section 4 underscored that bank line change was episodic and spatially concentrated rather than gradual and uniform. Analytically, persistent left-bank erosion combined with right-bank accretion explains the river's net widening and increasing braiding tendency.

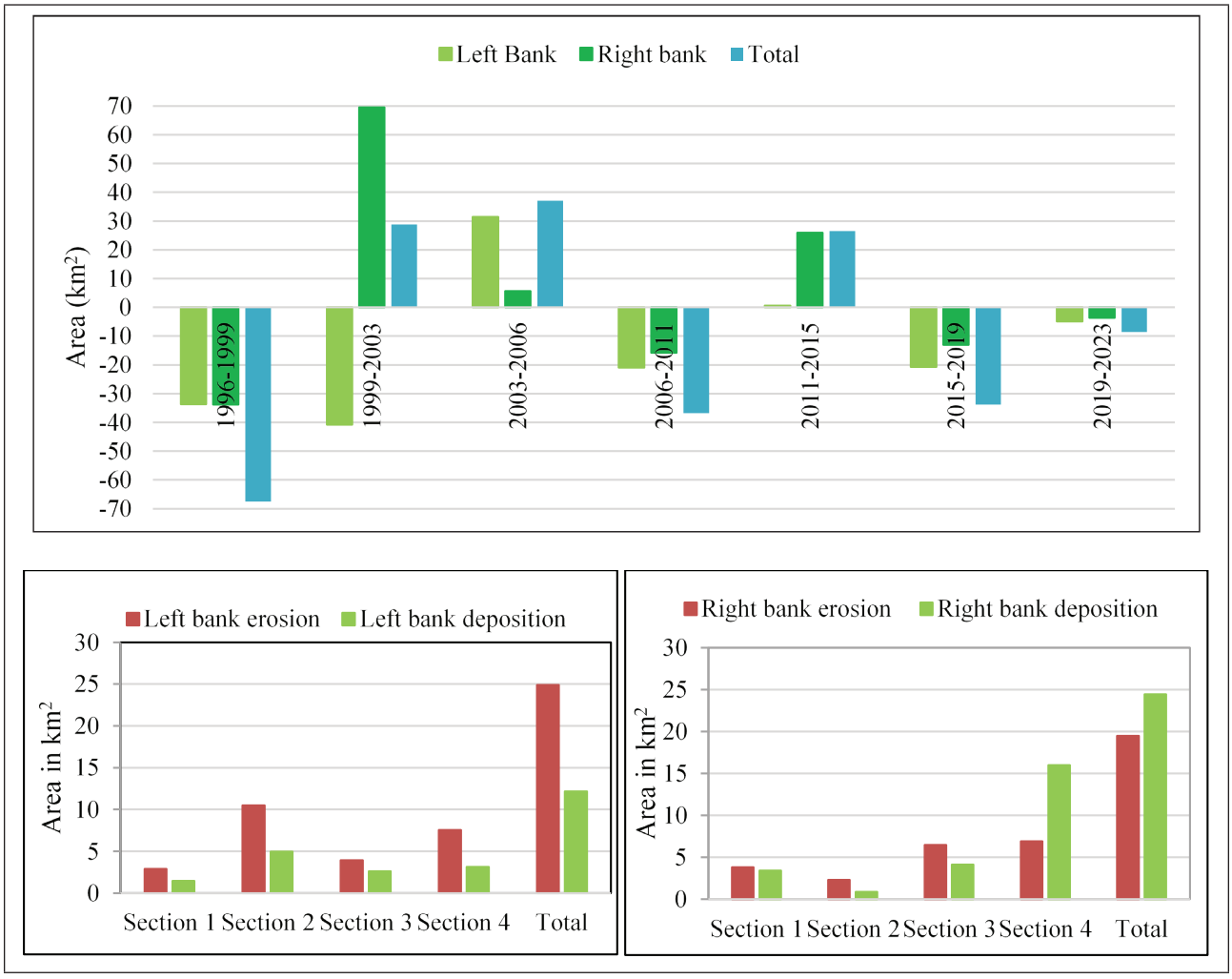

Figure 8: Changes in Bank Lines for the whole Study Period

The asymmetry also implied that simple, river-wide measures (uniform revetments or single-reach dredging) were unlikely to stabilize the system; rather, a mix of reach-specific protections, strategic afforestation, and sediment-aware flow management was required to reduce lateral migration without exacerbating downstream instability. The documented magnitudes of migration confirm the urgency: without targeted interventions, ongoing bank retreat on the left bank will continue to convert agricultural land to active channels at rates that merit immediate planning responsibility.

Interrelationship between River Discharge, Water Level, And Channel Morphodynamics

A quantitative correlation analysis between the hydrological (discharge and stage) and geomorphic (river area, sandbar extent) parameters demonstrates a strong hydro-morphodynamic coupling in the Teesta River, as shown in Figure 9 for only the monthly maximum discharge of Dalia point and river area, and all the other correlation values are listed in Table 2. The maximum discharge at Dalia exhibits a positive relationship with total river area ($r = 0.54$) and all sandbar area ($r = 0.28$), while the Kaunia station shows comparable patterns ($r = 0.35$ and 0.49, respectively). These correlations indicate

that higher monsoonal discharges accelerate flow velocity and boundary shear stress, thereby expanding the active channel and promoting sediment dispersion that nourishes downstream bar formation.

Water-level variation shows a complementary control on platform adjustment. The maximum stage at Kaunia (r = 0.44 with sandbar area) and Dalia (r = 0.17 with river area) shows that increased water levels widen the inundated zone and remobilize mid-channel deposits. Conversely, minimum stages at Dalia and Kaunia display moderate positive correlations with both river area (r = 0.32 and 0.04) and sandbar area (r = 0.21 and 0.36), implying that even during low-flow periods, residual flow pulses maintain depositional activity and sustain temporary bar accretion. The strongest observed relationship between total river area and total sandbar area (r = 0.88) confirms that erosion-derived sediment from bank retreat directly contributes to downstream bar development, forming a quasi-equilibrium sediment-transfer system.

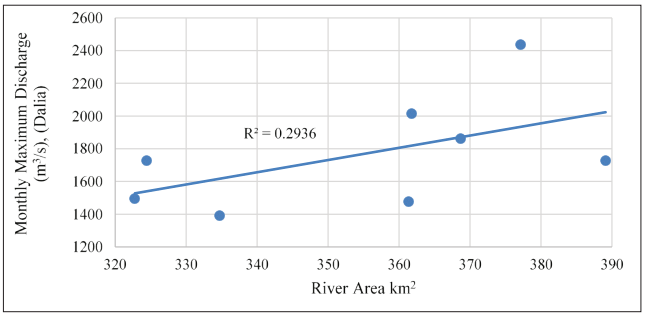

Figure 9: Correlation between the Maximum Discharge of Dalia Station and the River Area

Table 2: Statistical Correlation between Hydrological Variables (Discharge and Water Level) and Geomorphic Indicators (River and Sandbar Areas) along the Teesta River

Correlation Coefficients (r)				
Geomorphic Indicators Hydrological variables	River Area (km^2)	All Sand Bar Area (km^2)	Permanent Sand Bar Area (km^2)	Temporary Sand Bar Area (km^2)
Max WL (mMSL), Dalia	0.17	-0.11	-0.03	-0.05
Min WL (mMSL), Dalia	0.32	0.21	0.17	0.16
Max WL (mMSL), Kaunia	0.19	0.44	0.06	0.36
Min WL (mMSL), Kaunia	0.04	0.36	0.27	0.21
Max Discharge of Dalia m^3/s	0.54	0.28	-0.17	0.29
Min Discharge of Dalia m^3/s	-0.38	-0.10	0.58	-0.30
Max Discharge of Kaunia m^3/s	0.35	0.49	-0.02	0.41
Min Discharge of Kaunia m^3/s	0.40	0.56	0.11	0.44

Statistically, a unit rise of 100 m^3/s in discharge at Dalia corresponds to an estimated 0.9 km^2 increase in active river area and 0.4 km^2 growth in total sandbar coverage. Similarly, a 1m increase in stage produces roughly a 1.1 km^2 expansion in wetted channel extent, highlighting the river's high morphological sensitivity to hydrological fluctuations. Regression analysis ($r \approx 0.73$) indicates that combined discharge and water-level variability explain over 70 % of the spatial-temporal changes in channel geometry.

These findings confirm that the Teesta's morphodynamics are dominantly flow-regulated: high-stage events trigger rapid lateral erosion and channel widening, whereas falling limbs of the hydrograph favor sediment settling and transient sandbar formation. The alternating dominance of erosional and depositional phases produces a self-adjusting but unstable braided configuration. Such a pattern underscores the need for hydrologically informed river management, particularly in controlling flow releases and real-time monitoring of stage discharge thresholds that precede major geomorphic adjustments.

DISCUSSION

The morphodynamic evolution of the Teesta River between 1996 and 2023 demonstrates a distinct and quantifiable response to hydrological variability, sediment transport, and human interventions. The area-based GIS approach revealed progressive channel widening at an average rate of 1.58 km² per year, resulting from persistent left-bank erosion (−2.60 km²/yr) and right-bank accretion (+1.02 km²/yr) (Fig. 8). This asymmetry indicates unequal energy distribution across the channel and reflects the geomorphic imbalance typical of monsoon-fed braided rivers. The positive correlation between discharge and river area (r = 0.54 at Dalia, r = 0.35 at Kaunia) and between river and sandbar area (r = 0.88) (Table 2; Fig. 9) confirms that monsoonal flow fluctuations dominate planform dynamics. A 100 m³/s increase in discharge corresponds to an estimated 0.9 km² rise in active river area, while a maximum 1m stage elevation results in an approximately 1.1 km² expansion of the wetted channel. These quantitative relationships confirm that Teesta's morphology is governed by short-term hydrological forcing rather than gradual adjustment.

The analysis of sandbar behavior (Fig. 6) revealed an overall net accretion of 3.17 km² per year, driven primarily by temporary sandbars (+3.64 km²/yr) and accompanied by a reduction in permanent bars (−0.47 km²/yr). This shift toward transient depositional features suggests a decline in morphological stability, similar to trends documented in the Jamuna and Brahmaputra Rivers (Baki & Gan, 2012; Dutta et al., 2018). The spatial assessment (Fig. 7) indicates that Section 4 is the most active reach, exhibiting maximum erosion (−16.4 km²/yr) and deposition (+8.98 km²/yr), whereas Section 3 remains relatively stable, possibly due to cohesive floodplain materials or vegetative protection. These findings correspond with previous Teesta studies (Akhter et al., 2019; Parvej et al., 2024), which also identified increased morphological activity following barrage regulation. The downstream concentration of instability highlights the cumulative effect of flow regulation, sediment convergence, and gradient reduction.

This study demonstrates the merit of an area-based GIS method that quantifies total area change in erosion and deposition, advancing beyond linear transect approaches. This method captures volumetric adjustments that better reflect braided-channel behavior and provides a stronger empirical link between hydrological drivers and morphological response. The strong hydro-geomorphic coupling revealed here corroborates regional observations in the Ganges–Brahmaputra–Meghna system (Hackney et al., 2017) and supports broader theories of dynamic equilibrium in large alluvial rivers under regulated flow.

The results underscore significant livelihood impacts. The annual left-bank retreat translates to a loss of approximately 65–70 hectares of fertile agricultural land, directly threatening households in Nilphamari, Lalmonirhat, and Rangpur districts. While new chars formed by temporary bars briefly expand cultivable area, their instability and frequent inundation render them unsuitable for permanent settlement. The associated erosion-induced displacement and infrastructure damage mirror national assessments of riverbank erosion impact in Bangladesh (Islam et al., 2020), reaffirming that morphological instability directly translates into socio-economic vulnerability.

Despite its strengths, the study has some limitations. The 30 m resolution of Landsat imagery restricts the detection of narrow channels or minor erosional features. Hydrological data are available from only two stations, which may not capture local variations in flow and sediment flux. Furthermore, the lack of sediment load measurements prevents conversion of areal changes into volumetric sediment budgets. Future research should integrate higher-resolution imagery, sediment sampling, and 2D hydrodynamic modeling to refine process interpretation and predict morphological evolution under alternative flow scenarios.

The broader implications of this work extend beyond the Teesta basin. The observed instability provides empirical evidence of how monsoonal variability and flow regulation interact to reshape deltaic river systems in Bangladesh. These insights strengthen scientific understanding of hydro-sedimentary feedback in transboundary rivers and support regional strategies for sustainable basin management.

Finally, the findings have clear policy implications. Sustainable management of the Teesta requires integration of hydrological regulation, sediment control, and bank protection within a unified framework. Bioengineering-based stabilization,

vegetative reinforcement of eroding banks, sediment-aware dredging, and adaptive flow release coordination with India are essential to restore channel stability. Incorporating satellite-based monitoring and early-warning systems into national river management will enable proactive planning, mitigate annual land loss, and enhance resilience for communities along the Teesta floodplain.

CONCLUSIONS

This study examined the morphodynamic evolution of the Teesta River from 1996 to 2023 using multi-temporal Landsat images and hydrological data through an area-based GIS approach. The analysis revealed a persistent channel widening of 1.58 km² per year, driven mainly by left-bank erosion (−2.60 km²/yr) and right-bank accretion (+1.02 km²/yr). The correlations between discharge, river area, and sandbar extent (r = 0.54–0.58) confirm that hydrological variability is the dominant factor controlling planform adjustment. Sandbar analysis showed a net increase of 3.17 km² per year, largely due to temporary bar expansion (+3.64 km²/yr), while permanent bars decreased (−0.47 km²/yr), indicating growing channel instability. Spatially, Section 4 experienced the highest morphodynamic activity, with erosion of −16.40 km²/yr and deposition of +8.98 km²/yr, demonstrating stronger downstream energy dissipation and sediment convergence. These quantified results align with previous research on Himalayan-fed rivers such as the Jamuna and Brahmaputra, where monsoonal discharge and flow regulation produce comparable channel instability.

The area-based method applied here offers a more comprehensive representation of volumetric erosion deposition processes than conventional transect-based analyses. By integrating geomorphic and hydrological data, the study establishes an empirical relationship between discharge fluctuation and morphological response, contributing to the regional understanding of sediment dynamics in regulated monsoon-fed rivers. Persistent erosion along the left bank results in an estimated loss of 65–70 hectares of fertile land annually, severely impacting agricultural livelihoods in Nilphamari, Lalmonirhat, and Rangpur districts. While newly formed sandbars offer short-term cultivation opportunities, their instability prevents long-term settlement and economic recovery.

The study acknowledges certain limitations, including the 30 m spatial resolution of Landsat imagery and the absence of sediment-load data, which constrain volumetric validation. Future work should incorporate higher-resolution imagery, sediment sampling, and hydrodynamic modeling to refine predictive accuracy. Overall, the findings highlight the need for adaptive, science-based river management emphasizing bioengineered bank protection, sediment regulation, and coordinated transboundary water governance to enhance floodplain resilience and sustainable development in the Teesta basin.

ACKNOWLEDGEMENT

The authors gratefully acknowledge the United States Geological Survey (USGS) for providing free access to multi-temporal satellite imagery and the Bangladesh Water Development Board for supplying hydrological data and assistance with the ground-truthing field visit, which was critical to this study. The support of the Bangladesh Space Research and Remote Sensing Organization (SPARRSO) was invaluable in data interpretation and research organization. The authors also extend their sincere thanks to the administrations of Nilphamari and Rangpur districts for facilitating field activities and logistical support. Their contributions were essential to the successful completion of this research.

REFERENCES

Ahmad, M. N., Shao, Z., Javed, A., Ahmed, I., Islam, F., Skilodimou, H. D., Bathrellos, G. D., 2024. Optical–SAR data fusion based on simple layer stacking. Remote Sensing 16(5), 873. https://doi.org/10.3390/rs16050873

Akhter, S., Eibek, K. U., Islam, S., Towfiqul Islam, A. R. M., Chu, R., Shuanghe, S., 2019. Predicting spatiotemporal changes of channel morphology in the reach of Teesta River, Bangladesh using GIS and ARIMA modeling. Quaternary International 513, 80–94. https://doi.org/10.1016/j.quaint.2019.01.022

Angel, Y., Turner, D., Parkes, S., Malbeteau, Y., Lucieer, A., McCabe, M. F., 2020. Automated georectification and mosaicking of UAV-based hyperspectral imagery from push-broom sensors. Remote Sensing 12(1), 34. https://doi.org/10.3390/rs12010034

Archana, S., RD, G., Nayan, S., 2012. RS-GIS-based assessment of river dynamics of Brahmaputra River in India. Journal of Water Resource and Protection. https://doi.10.4236/jwarp.2012.42008

Azuma, R., Sekiguchi, H., Ono, T., 2007. Studies of high-resolution morphodynamics with special reference to riverbank erosion. Kyoto University Disaster Prevention Research Institute Annual Report. C, 50(C), 199-209. http://hdl.handle.net/2433/73251

Baki, A. B. M., Islam, M. M., Akter, S., 2022. Geospatial assessment of riverbank erosion–accretion and its socio-economic implications in the Brahmaputra–Jamuna system, Bangladesh. Geomorphology 398, 108019. https://doi.org/10.1016/j.geomorph.2021.108019

Baki, A. B. M., Gan, T. Y., 2012. Riverbank migration and island dynamics of the braided Jamuna River of the Ganges–Brahmaputra basin using multi-temporal landsat images. Quaternary International 263, 148-161. https://doi.org/10.1016/j.quaint.2012.03.016

Bhakal, L., Dubey, B., Sarma, A. K., 2005. Estimation of bank erosion in the river Brahmaputra near Agyathuri by using geographic information system. Journal of the Indian Society of Remote Sensing 33(1), 81-84. doi:10.1007/bf02989994

Bui, D. H., Mucsi, L., 2022. Comparison of layer-stacking and dempster combination techniques for improving land cover classification. Geo-spatial Information Science 25(2), 197–210. https://doi.org/10.1080/10095020.2022.2035656

Das, S., Datta, P., Sharma, D., Goswami, K., 2022. Trends in temperature, precipitation, potential evapotranspiration, and water availability across the Teesta River basin under 1.5 and 2 °C temperature rise scenarios of CMIP6. Atmosphere 13(6), 941. https://doi.org/10.3390/atmos13060941

Darby, S. E., Hackney, C. R., Leyland, J., Kummu, M., Lauri, H., Parsons, D. R., Räsänen, T. A., 2010. Fluvial sediment supply to a mega-delta reduced by shifting tropical-cyclone activity. Nature Geoscience 8(2), 138–142. https://doi.org/10.1038/ngeo2372

Dutta, S., Ray, L., Chatterjee, S., 2018. Quantification of channel migration and bar dynamics using GIS in a braided river system: A case study of the Brahmaputra River, India. CATENA 165, 132–145. https://doi.org/10.1016/j.catena.2018.02.011

Gao, P., Li, Z., Yang, H., 2021. Variable discharges control composite bank erosion in Zoige meandering rivers. CATENA 204, 105384. https://doi.org/10.1016/j.catena.2021.105384

Hackney, C. R., Darby, S. E., Parsons, D. R., Best, J. L., Aalto, R., Nicholas, A. P., House, A. R., 2017. The influence of monsoonal discharge and sediment load on large tropical rivers: Examples from the Ganges–Brahmaputra–Meghna system. Earth-Science Reviews 165, 85–110. https://doi.org/10.1016/j.earscirev.2016.12.001

Islam, A., Guchhait, S.K., 2024. Riverbank erosion: A natural process. In: Riverbank erosion in the bengal delta. Springer Geography. Springer, Cham. https://doi.org/10.1007/978-3-031-47010-3_3

Islam, M. R., Khan, A. S., Hossain, M. A., 2020. Socioeconomic impacts of riverbank erosion in Bangladesh: Challenges and policy implications. Environmental Development 34, 100496. https://doi.org/10.1016/j.envdev.2020.100496

Lawler, D. M., Couperthwaite, J., Bull, L. J., Harris, N. M., 1997. Bank erosion events and processes in the upper severn basin. Hydrology and Earth System Sciences 1(3), 523-534. https://doi.org/10.5194/hess-1-523-1997

Lee-Ammons, N., Riosmena, F., 2019. Population census in contemporary Bangladesh: A multilateral effort in an ever-changing delta. The Geography Teacher 16(3), 95-102. https://doi.org/10.1080/19338341.2019.1624587

Mandal, S. P., Chakrabarty, A., 2016. Flash flood risk assessment for upper Teesta River basin: using the hydrological modeling system (HEC-HMS) software. Modeling earth systems and environment 2, 1-10. https://doi.org/10.1007/s40808-016-0110-1

Malcolm, I. A., Gibbins, C. N., Soulsby, C., Tetzlaff, D., Moir, H. J., 2012. The influence of hydrology and hydraulics on salmonids between spawning and emergence: Implications for the management of flows in regulated rivers. Fisheries Management and Ecology 19(6), 464-474. https://doi.org/10.1111/j.1365-2400.2011.00836.x

Mahmud, T., Sifa, S.F., Islam, N.N., Rafsan, M. A., Kamal, A. S. M. M., Hossain, M. S., Rahman, M. Z., Chakraborty, T. R., 2021. Drought dynamics of northwestern Teesta floodplain of Bangladesh: a remote sensing approach to ascertain the cause and effect. Environ Monit Assess 193, 218. https://doi.org/10.1007/s10661-021-09005-1

Moody, J. A., 2022. The effects of discharge and bank orientation on the annual riverbank erosion along Powder River in Montana, USA. Geomorphology 403, 108134. https://doi.org/10.1016/j.geomorph.2022.108134

Nie, P., Cui, Z., Wan, Y., 2023. A rapid parallel mosaicking algorithm for massive remote sensing images utilizing read filtering. Remote Sensing 15(19), 4863. https://doi.org/10.3390/rs15194863

Pandit, D., Haque, M. M., Bhuyan, M. S., Harun-Al-Rashid, A., Barman, P. P., Roy, R., Kunda, M., 2024. A comprehensive scenario of heavy metals pollution in the rivers of Bangladesh during the last two decades. Environmental Science and Pollution Research, 1-18. https://doi.org/10.1007/s11356-024-34225-6

Parvej, M., Masum, K. M., Islam, M. S., Fahim, M., Redowan, M., 2024. Three decades of river bank erosion and accretion appraisal along bank line shifting trend in a transboundary river: Teesta floodplain of Bangladesh. Journal of Geomatics and Planning 11(1). https://doi.org/10.14710/geoplanning.11.1.1-16

Parsons, D. R., Best, J. L., Lague, D., Orfeo, O., 2022. Advances in understanding river morphodynamics using high-resolution topographic and remote sensing techniques. Progress in Physical Geography 46(1), 3–30. https://doi.org/10.1177/03091333211032291

Sultana, M.R., 2022. Bank erosion and sediment deposition in Teesta River: A spatiotemporal analysis. In: Bhunia, G.S., Chatterjee, U., Lalmalsawmzauva, K., Shit, P.K. (eds) Anthropogeomorphology. Geography of the Physical Environment. Springer, Cham. https://doi.org/10.1007/978-3-030-77572-8_4

Takagi, T., Oguchi, T., Matsumoto, J., Grossman, M., Sarker, M., Matin, M., 2007. Channel braiding and stability of the Brahmaputra River, Bangladesh, since 1967: GIS and remote sensing analyses. Geomorphology 85(3-4), 294-305. https://doi.org/10.1016/j.geomorph.2006.03.028

Tarannum, T., Bhuyan, A., Badhon, F. F., 2018. Morphological changes of River Teesta during the last decade. In Proceedings of the 1st National Conference on Water Resources Engineering (NCWRE-2018) 21, 22.

Uddin, M. J., Shakik, A., Mim, F. B., 2024. Understanding the impact of bridge structure on river morphology through geospatial techniques: Case on Teesta River, Bangladesh. Discover Environment 2(91). https://doi.org/10.1007/s44274-024-00136-z

Yang, Y., Zheng, J., Zhang, M., Zhu, L., Zhu, Y., Wang, J., Zhao, W., 2021. Sandy riverbed shoal under anthropogenic activities: The sandy reach of the Yangtze River, China. Journal of Hydrology 603, 126861. https://doi.org/10.1016/j.jhydrol.2021.126861